Effects of flow shear and Alfvén waves on two-dimensional magnetohydrodynamic turbulence

Jamie Douglas,[1] Eun-jin Kim,[1] and A. Thyagaraja[2]
[1]*Department of Applied Mathematics, University of Sheffield, Sheffield, S3 7RH, United Kingdom*
[2]*EURATOM/UKAEA Fusion Association, Culham Science Centre, Abingdon, OX14 3DB, United Kingdom*

(Received 30 January 2008; accepted 3 April 2008; published online 15 May 2008)

The suppression of turbulent transport by large scale mean shear flows and uniform magnetic fields is investigated in two-dimensional magnetohydrodynamic turbulence driven by a small-scale forcing with finite correlation time. By numerical integration the turbulent magnetic diffusivity D_T is shown to be significantly quenched, with a scaling $D_T \propto B^{-2}\Omega_0^{-5/4}$, which is much more severe than in the case of a short or delta correlated forcing typified by white noise, studied in E. Kim and B. Dubrulle [Phys. Plasmas **8**, 813 (2001)]. Here B and Ω_0 are magnetic field strength and flow shear rate, respectively. The forcing with finite correlation time also leads to much stronger suppression of momentum transport through the cancellation of the Reynolds stress by the Maxwell stress with a positive small value of turbulent viscosity, $\nu_T > 0$. While fluctuating kinetic and magnetic energies are unaffected by the magnetic field just as in the case of a delta correlated forcing, they are much more severely quenched by flow shear than in that of a delta correlated forcing. Underlying physical mechanisms for the reduction of turbulent transport and turbulence level by flow shear and magnetic field are discussed. © *2008 American Institute of Physics*. [DOI: 10.1063/1.2913270]

I. INTRODUCTION

Turbulence has a major impact on transport in any turbulent fluid system. Specifically, the turbulent transport coefficients are normally several orders of magnitude larger than the collisional values, leading to a significant alteration in the overall transport in the system. This enhanced transport due to turbulence has often been invoked to explain rapid magnetic dissipation (e.g., solar coronal heating, major disruptions in tokamaks, etc.), particle mixing, or momentum transport observed in astrophysical and laboratory plasmas. For instance, the turbulent (anomalous) magnetic field diffusivity is often estimated to be $D_T \sim vl$ where v and l are the characteristic amplitude and length scale of the velocity of the turbulent flow, much larger than the magnetic diffusivity $D = \eta/\mu_0$ based on Ohmic resistivity $\eta = \eta_{\text{Spitzer}}$ given by the Spitzer value. However, recent works such as Refs. 1–3 have shown that turbulent magnetic diffusivity is quenched in two-dimensional (2D) magnetohydrodynamics (MHD) due to magnetic back reaction (i.e., Lorentz force) which changes random turbulent motion to more coherent wavelike Alfvénic turbulence where the fluctuating magnetic field $\mathbf{b}'$ tends to align with fluctuating velocity $\mathbf{v}'$ (i.e., $\mathbf{b}' \sim \pm \mathbf{v}'$), supporting the propagation of Alfvén waves. This process is referred to as Alfvénization. Especially, the quenching is very severe for a system of large-size with large magnetic Reynolds number $Rm = vl/D$ with scaling $D_T \propto Rm^{-1/2}B^{-2}$, where B is the large scale magnetic field, as shown in Ref. 2. The Alfvénization of turbulence due to magnetic field also has a dramatic effect on momentum transport (see, for example, Ref. 3). That is, not only can it modify its magnitude through the cancellation of Reynolds stress by Maxwell stress, but also changes the direction of the energy cascade. Note that the direction of the energy cascade determines whether energy is transferred from large scale flows to small scale turbulence in the case of a direct cascade, or from small scale turbulence up to large scale flows in the case of an inverse cascade (i.e., whether large-scale flows grow or decay due to turbulence), while the magnitude of momentum transport controls the rate of this cascade. The prediction of momentum transport is thus crucial for understanding the origin and evolution of large-scale flows which are ubiquitous in a variety of systems, including the Earth's atmosphere and oceans, other planetary atmospheres, differential rotation in stars (e.g., the solar tachocline where large scale shear flows arise due to radial differential rotation) and in laboratory plasmas.

In particular, laboratory plasmas such as tokamak plasmas and the plasmas of other fusion devices support both zonal flows resulting from the turbulence itself and also mean shear flows driven by mean pressure gradients (see, for example, Refs. 4 and 5). These shear flows can reduce turbulent transport dramatically by shear flow suppression, as shown in Refs. 4, 6, and 7, leading to the formation of transport barriers. This is due to the distortion and disruption of turbulent eddies by flow shear, as described in Refs. 3 and 8, which preferentially elongates an eddy along the shear flow. This not only inhibits the transport in the direction of the flow shear by directly hindering the motion, but also rapidly generates fine scales in that direction, speeding up the dissipation of eddies followed by their break up (the so-called enhanced dissipation; see Ref. 9). A notable example of the formation of transport barriers by flow suppression is the transition from the low to high confinement regimes (L-H transition), which has received considerable experimental support (see, for example, Ref. 4).

Given the common occurrence of shear flows in magnetized plasmas, the investigation of how a shear flow as well as a magnetic field affects turbulent transport is essential for understanding and prediction of transport in these systems.

 © 2008 American Institute of Physics

Downloaded 10 Aug 2011 to 194.81.223.66. Redistribution subject to AIP license or copyright; see http://pop.aip.org/about/rights_and_permissions

For instance, should there be a similar reduction of dissipation of magnetic fields, there would then be an impact, amongst others, on the idea of turbulent magnetic diffusion as a mechanism for dissipation of magnetic fields on a time scale massively shorter than the Ohmic diffusive one. Further, the predicted value of turbulent momentum flux will shed light on the efficiency of momentum transport as well as the direction of the energy cascade (i.e., whether shear flows such as zonal flows form or decay due to turbulence) in these systems.

The purpose of this paper is to calculate turbulent transport coefficients in magnetized plasmas in the presence of mean shear flows as a means to determine the transport properties of these systems. The principle objective is to investigate the role of flow shear and Alfvén waves in the quenching of turbulence and transport by considering the stable equilibrium provided by a stable large-scale shear flow and uniform magnetic field which are parallel to each other. The latter ensures that there is no direct interaction between (steady) equilibrium shear flow and magnetic field such as phase mixing discussed in Refs. 10–12, thereby permitting us to focus on the study of their indirect effects on transport through the modification of turbulence. The calculation of turbulent viscosity and turbulent diffusivity will enable the quantitative prediction for turbulent transport reduction (or enhancement) due to shear flows and magnetic field strength separately. With these predictions other physical processes for enhanced transport may be proposed to explain observed phenomena involving fast transport.

The case of a temporally short correlated forcing was studied analytically in Refs. 3 and 13 with the following key results. In a pure 2D hydrodynamic (HD) flow the turbulent viscosity is suppressed by shear flow with shear strength Ω_0 as Ω_0^{-2} in the strong shear limit. The turbulent viscosity is negative with an inverse cascade in HD turbulence. In the case of 2D MHD, turbulent diffusivity of magnetic fields is suppressed by both uniform magnetic field and shear as $\Omega_0^{-2/3}B^{-2}$ in the limit of both strong shear and magnetic field. Turbulent viscosity in this case is significantly reduced due to the cancellation of the Reynolds stress by the Maxwell stress due to the Alfvénization of fluid motion, with the resulting turbulent viscosity suppressed by magnetic field as B^{-2}. Note that the reduction of turbulent diffusivity by a factor of B^{-2} in a turbulent 2D MHD flow is in agreement with other previous works; see Refs. 1 and 2.

In this paper we extend the study of Refs. 3 and 13 to accommodate a forcing of finite frequency and memory time, and investigate how shear and magnetic field affect the transport coefficients by numerical calculation for a range of values of both shear and magnetic field strength. In addition to the relevance of finite correlated flows in real systems where turbulence is influenced by waves (e.g., the solar tachocline and fusion devices), the extension allows the investigation of the effect of resonance on transport that can enhance turbulent transport, similar to that studied in Ref. 14. In the limit of temporally short correlated forcing our numerical calculations confirm the key analytical results of Ref. 3. In general, for a forcing which has a finite frequency and correlation time, despite the resonance between turbulence and waves the transport is found to be more severely suppressed by the large-scale shear flow in the cases of both 2D HD and MHD turbulence. In the HD case, turbulent viscosity suppressed as Ω_0^{-2} in the delta correlated case is further suppressed as $\Omega_0^{-3}\ln\Omega_0$ in the case of a finite correlated forcing, while the inverse cascade remains unchanged. In the MHD case, the further reduction in momentum transport through a smaller value of turbulent viscosity in a flow is found with $\nu_T>0$ (i.e., direct energy cascade). Magnetic diffusivity is found to be severely quenched due to shear and magnetic field as $\Omega_0^{-5/4}B^{-2}$, with a stronger reduction due to shear than in the case of a delta correlated forcing.

The remainder of the paper is structured as follows: The formulation of the problem is provided in Sec. II. The main governing equations and results for the HD case are presented and discussed in Sec. III and for the MHD case (including turbulent viscosity and turbulent diffusivity) in Sec. IV, respectively. A conclusion is provided in Sec. V.

II. FORMULATION

We consider a viscoresistive incompressible MHD fluid stirred by an external incompressible small-scale forcing $\mathbf{F}$ in the presence of a uniform guide magnetic field aligned with shear flow. The velocity $\mathbf{v}$ and magnetic field $\mathbf{b}$ are governed by the Navier–Stokes and induction equations, respectively, constrained by the incompressible and solenoidal conditions,

$$\rho\left(\frac{\partial}{\partial t}+\mathbf{v}\cdot\nabla\right)\mathbf{v}=-\nabla p+\frac{1}{\mu_0}(\nabla\times\mathbf{b})\times\mathbf{b}+\mu\nabla^2\mathbf{v}+\mathbf{F}, \tag{1}$$

$$\frac{\partial\mathbf{b}}{\partial t}=\nabla\times(\mathbf{v}\times\mathbf{b})+\frac{\eta}{\mu_0}\nabla^2\mathbf{b}, \tag{2}$$

$$\nabla\cdot\mathbf{v}=\nabla\cdot\mathbf{b}=0. \tag{3}$$

Here, p is the scalar pressure, ρ is the mass density, μ is the collisional (Braginskii) viscosity due to ion-ion collisions, η is the Ohmic resistivity, and μ_0 is the permeability of free space. We now introduce $V_A^2=B^2/\rho\mu_0$ as the Alfvén velocity, where B is the (fixed) magnitude of the equilibrium magnetic field. The magnetic field can be normalized by setting $\mathbf{b}^*=\mathbf{b}/B$, the velocity field similarly as $\mathbf{v}^*=\mathbf{v}/V_A$. Furthermore we introduce nondimensional space and time variables $\mathbf{x}^*=\mathbf{x}/L_z$ and $t^*=tV_A/L_z$, where L_z is the assumed finite characteristic length scale of the system in the z direction. We now nondimensionalize the system of Eqs. (1)–(3) by dividing Eq. (1) by ρV_A^2, dividing Eq. (2) by V_A^2, and dividing the incompressible and solenoidal constraints by V_A and $\sqrt{(\rho\mu_0)}V_A$, respectively. This gives

$$\left(\frac{\partial}{\partial t^*}+\mathbf{v}^*\cdot\nabla^*\right)\mathbf{v}^*=-\nabla^*p^*+(\nabla^*\times\mathbf{b}^*)\times\mathbf{b}^*+\nu\nabla^{*2}\mathbf{v}^*+\mathbf{F}^*, \tag{4}$$

$$\frac{\partial\mathbf{b}^*}{\partial t^*}=\nabla^*\times(\mathbf{v}^*\times\mathbf{b}^*)+D\nabla^{*2}\mathbf{b}^*, \tag{5}$$

Downloaded 10 Aug 2011 to 194.81.223.66. Redistribution subject to AIP license or copyright; see http://pop.aip.org/about/rights_and_permissions

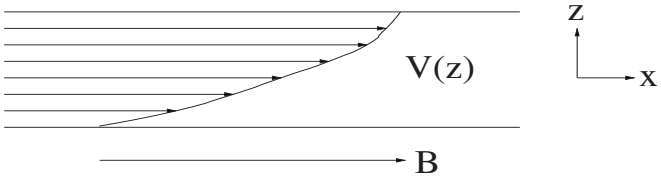

FIG. 1. The configuration of the large scale shear flow and magnetic field.

$$\nabla^* \cdot \mathbf{v}^* = \nabla^* \cdot \mathbf{b}^* = 0, \tag{6}$$

where $\nu = \mu/\rho V_A L_z$ is the nondimensional kinetic viscosity, $p^* = p/\rho V_A^2$ is the nondimensional pressure, $\mathbf{F}^* = \mathbf{F}/\rho V_A^2$ is the nondimensional forcing, $D = \eta/\mu_0 V_A L_z$ is the nondimensional magnetic diffusivity, and the starred differential operators represent derivatives with respect to the nondimensional space variables. Note that the quantity $1/D = \mu_0 V_A L_z/\eta$ is the magnetic Reynolds number using the Alfvén velocity, also known as the Lundqvist number S. As all quantities are now dimensionless the stars are henceforth dropped.

In 2D (x,z), Eqs. (4) and (5) can be written in terms of the magnetic vector potential a and vorticity Ω, where $\mathbf{b} = (b_x, 0, b_z) = \nabla \times a\hat{\mathbf{y}} = (-\partial a/\partial z, 0, \partial a/\partial x)$ and $\Omega\hat{\mathbf{y}} = \nabla \times \mathbf{v} = \nabla \times (v_x, 0, v_z) = (\partial v_z/\partial x - \partial v_x/\partial z)\hat{\mathbf{y}}$, which are governed by the following equations:

$$\left(\frac{\partial}{\partial t} + \mathbf{v} \cdot \nabla\right)\Omega = -(\mathbf{b} \cdot \nabla)\nabla^2 a + \nu \nabla^2 \Omega + f, \tag{7}$$

$$\left(\frac{\partial}{\partial t} + \mathbf{v} \cdot \nabla\right) a = D\nabla^2 a. \tag{8}$$

Here $f\hat{\mathbf{y}} = \nabla \times \mathbf{F}$. The equilibrium is provided by stable shear flow $V(z)\hat{\mathbf{x}}$ and uniform magnetic field $\mathbf{B} = B\hat{\mathbf{x}}$ which is current free. By assuming that these background mean fields vary over a scale L and fluctuations over a characteristic scale l with a clear scale separation ($\epsilon = l/L \ll 1$), we separate $\mathbf{v}$ and $\mathbf{b}$ into their mean and fluctuating parts as follows:

$$\begin{aligned} \mathbf{v} &= \langle \mathbf{v} \rangle + \mathbf{v}' = \mathbf{V} + \mathbf{v}', \quad \Omega = \langle \Omega \rangle + \Omega' = \Omega_0 + \Omega', \\ \mathbf{b} &= \langle \mathbf{b} \rangle + \mathbf{b}' = \mathbf{B} + \mathbf{b}', \quad a = \langle a \rangle + a' = A + a'. \end{aligned} \tag{9}$$

Here the angular brackets represent averages over the statistics of the random forcing $\mathbf{F}$, giving the large scale fields, while the dashed variables are the small scale fields (and $\langle a' \rangle = 0$ always). Note that the large scale background magnetic potential is given by $\langle a \rangle = A = A(z)$.

The equilibrium shear flow is envisioned to be maintained by an external source which balances the dissipative terms in the absence of the small scale forcing. Therefore, large-scale vorticity and magnetic field are given by $\Omega_0 = -\partial V/\partial z$ and $\mathbf{B} = B\hat{\mathbf{x}} = -\partial A/\partial z\hat{\mathbf{x}}$. The domain in assumed to be finite with finite system size L_z in the z-direction while periodic in the x-direction. This is represented in Fig. 1.

In the following, we use quasilinear analysis by ignoring the nonlinear local interaction between fluctuations compared to nonlocal interaction between large and small scale fields. This is well justified for strongly sheared turbulence where the shear flow has the effect of quenching turbulence as a result of shearing, distortions, and disruption of turbulent eddies (as noted previously), making local interactions between small-scale flows negligible compared to nonlocal interactions. The prediction of quasilinear analysis for turbulent transport and turbulence level of passive scalar fields was numerically confirmed by Leconte *et al.*; see Ref. 15. The linear equations for fluctuations Ω' and a' are the following:

$$\left[\frac{\partial}{\partial t} + V\frac{\partial}{\partial x} - \nu\left(\frac{\partial^2}{\partial x^2} + \frac{\partial^2}{\partial z^2}\right)\right]\Omega' = -B\frac{\partial}{\partial x}\left(\frac{\partial^2}{\partial x^2} + \frac{\partial^2}{\partial z^2}\right)a' + f, \tag{10}$$

$$\left[\frac{\partial}{\partial t} + V\frac{\partial}{\partial x} - D\left(\frac{\partial^2}{\partial x^2} + \frac{\partial^2}{\partial z^2}\right)\right]a' = -v_z'\frac{\partial A}{\partial z}. \tag{11}$$

The mean field equations for V and A are found by taking the average of Eqs. (7) and (8) as follows:

$$\left[\frac{\partial}{\partial t} + V\frac{\partial}{\partial x} - \nu\frac{\partial^2}{\partial z^2}\right]V = -\frac{\partial}{\partial x}\left\langle p + \frac{b'^2}{2}\right\rangle - \frac{\partial}{\partial z}\langle v_x' v_z' - b_x' b_z' \rangle, \tag{12}$$

$$\left[\frac{\partial}{\partial t} + V\frac{\partial}{\partial x} - D\frac{\partial^2}{\partial z^2}\right]A = -\frac{\partial}{\partial z}\langle a' v_z' \rangle. \tag{13}$$

The total stress, $\langle v_x' v_z' - b_x' b_z' \rangle$ in Eq. (12), which is the difference between the Maxwell stress and the Reynolds stress, is an effective force on V which can be written as a turbulent viscous force by using a turbulent viscosity ν_T defined by

$$\langle v_x' v_z' - b_x' b_z' \rangle = -\nu_T \partial V/\partial z = \nu_T \Omega_0, \tag{14}$$

where $-\partial V/\partial z = \Omega_0$. This turbulent viscosity may be combined with the kinetic viscosity to give an effective viscosity $\nu + \nu_T$, as can be seen by direct substitution of Eq. (14) in Eq. (12). This effective viscosity can take any sign, being negative in the case of an inverse cascade and positive in the case of a direct cascade. It is worth pointing out that molecular values of transport coefficients are normally insignificant in comparison to the turbulent values so that the sign of ν_T entirely determines the direction of energy cascade in most applications.

On the other hand, the correlation $\langle a' v_z' \rangle$ in Eq. (13) gives a turbulent diffusivity D_T defined by

$$\langle a' v_z' \rangle = -D_T \partial A/\partial z = D_T B. \tag{15}$$

The substitution of Eq. (15) in Eq. (13) gives the effective diffusivity $D + D_T$; $D_T > 0$ represents an enhancement of the magnetic diffusivity.

The computation of ν_T and D_T in Eqs. (14) and (15) requires the solution for Ω' and a' and the evaluation of the correlation functions $\langle v_x' v_z' - b_x' b_z' \rangle$ and $\langle a' v_z' \rangle$. The solutions for Ω' and a' are provided in Ref. 3 in both the HD case with $B = 0$ and in the MHD case, specifically by nonperturbatively incorporating the effect of shear flow Ω_0. Although this was done in Ref. 3 by using the Gabor transform, in this paper we use a Fourier transform with time dependent wavenumber $k_z(t) = k_z(0) + k_x \Omega_0 t$ to capture the shearing effect, as done in Ref. 7. In contrast to Ref. 3, the correlation function

Downloaded 10 Aug 2011 to 194.81.223.66. Redistribution subject to AIP license or copyright; see http://pop.aip.org/about/rights_and_permissions

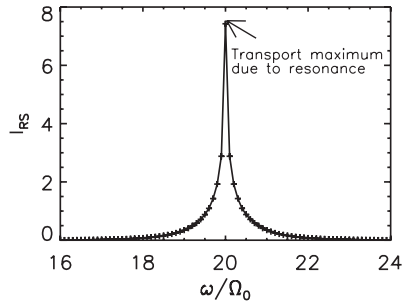

FIG. 2. I_{RS} in Eq. (19) plotted against normalized turbulent frequency $\bar{\omega}=\omega/\Omega_0$. A resonant peak of maximum transport when $\omega/\Omega_0=k_x$ can be seen.

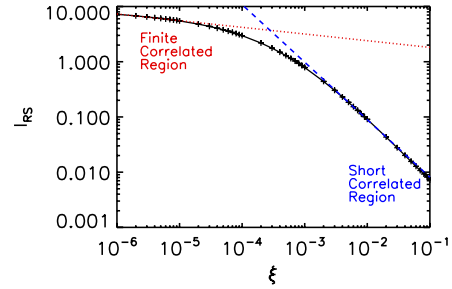

FIG. 3. (Color online) Dependence of I_{RS} in Eq. (19) on shearing rate $\xi \propto \Omega_0^{-1}$.

of forcing here is assumed to have a finite memory time $\tau_c=\gamma^{-1}$ and frequency ω. Specifically we assume spatially homogeneous and temporally stationary forcing with the following correlation function for Fourier transform $\hat{F}$:

$$\langle \hat{F}(\mathbf{k}_1,t_1)\hat{F}(\mathbf{k}_2,t_2)\rangle = (2\pi)^2\delta(\mathbf{k}_1+\mathbf{k}_2)\tilde{\phi}(\mathbf{k}_2,t_2-t_1), \quad (16)$$

with the following power spectrum $\tilde{\phi}$:

$$\tilde{\phi}(\mathbf{k}_2,t_2-t_1) = \hat{\phi}(\mathbf{k}_2)e^{-i\omega(t_2-t_1)-\gamma|t_2-t_1|}. \quad (17)$$

Note that exact solutions to the initial value problem with shear flow can also be obtained by using the Laplace transform; see Ref. 10.

Using these governing equations and key assumptions, we derive the equations for the correlation functions $\langle v_x' v_z'\rangle$, $\langle b_x' b_z'\rangle$ and $\langle a' v_z'\rangle$ and numerically compute their dependence on the shearing rate and magnetic field strength in the next sections. By using the definitions (14) and (15), we then determine the dependence of the transport coefficients (turbulent viscosity and turbulent magnetic diffusivity) on shear and magnetic field.

III. HYDRODYNAMICS

It is instructive to examine the effect of shear and resonance on transport in 2D HD by using a general forcing given by Eq. (16). To this end we first consider the case $B=0$ and calculate the momentum transport by using the solution given by Eq. (26) in Ref. 3, together with the correlation function given in Eqs. (16) and (17) obtaining the following Reynolds stress:

$$\langle v_x' v_z'\rangle = -\frac{1}{(2\pi)^2\Omega_0^2}\int d\mathbf{k}\frac{\hat{\phi}(\mathbf{k})}{k_x^2}e^{2\xi[k_z/k_x+1/3(k_z/k_x)^3]}I_{RS}, \quad (18)$$

where I_{RS} is defined as

$$I_{RS} = \int_0^\infty\int_0^\infty d\tau_2 d\tau_1 \frac{\tau_2}{[1+\tau_1^2][1+\tau_2^2]} \times e^{\{i(\bar{\omega}-k_x)(\tau_2-\tau_1)-\bar{\gamma}|\tau_2-\tau_1|-\xi[Q(\tau_1)+Q(\tau_2)]\}}. \quad (19)$$

Here, $\xi=\nu k_x^2/\Omega_0$ is a factor inversely proportional to the shear strength, $\mathbf{k}=(k_x,0,k_z)$ and $Q(\tau)$ is defined to be $Q(\tau)=\tau+\tau^3/3$. In Eq. (19), time t is normalized by shearing rate Ω_0 as $\tau=t\Omega_0$, turbulent frequency as $\bar{\omega}=\omega/\Omega_0=\xi\hat{\omega}$, and decorrelation rate as $\bar{\gamma}=\xi\hat{\gamma}$, where $\xi=\nu k_x^2/\Omega_0$, $\hat{\omega}=\omega/\nu k_x^2$ and $\hat{\gamma}=\gamma/\nu k_x^2$. Note that $\xi \ll 1$ represents the limit of strong shear, while $\xi \gg 1$ is the limit of weak shear.

In order to determine how shear flow affects the momentum flux, and therefore the turbulent viscosity, I_{RS} in Eq. (19) is numerically computed using an extended Simpsons rule algorithm (see Ref. 16) repeated over the integrals of both τ_2 and τ_1 up to a value of τ_i for $i=1,2$ at which each integral has converged. This is done for a range of values of shear strength. Figure 2 shows I_{RS} as a function of $\bar{\omega}=\omega/\Omega_0$ for the fixed values of $\xi=10^{-6}$, $k_x=20.0$, and $\hat{\gamma}=10^{-2}$. The peak in Fig. 2 occurs at the resonance $\omega=k_x\Omega_0$ where Doppler shifted frequency $(\omega-k_x\Omega_0)$ vanishes. In the following numerical calculation of I_{RS} for different values of ξ, the value of the turbulent frequency ω is thus chosen to be the value which gives maximum I_{RS} (momentum transport) due to this resonance.

Figure 3 shows the result of the numerical integration of I_{RS} for a fixed wavenumber $k_x=20.0$ and decorrelation rate $\hat{\gamma}=10^2$ over the range $10^{-6}<\xi<10^{-1}$. The dashed line is the asymptotic fit for larger values of $\xi>10^{-3}$ corresponding to weak shear limit and a short correlated forcing of the flow, which scales as ξ^{-1}. Note that in this region there is no resonance. The multiplicative factor Ω_0^{-2} outside I_{RS} in Eq. (19), together with Eq. (14) then gives turbulent viscosity as $\nu_T \propto \Omega_0^{-2}$. This scaling is in agreement with the analytic work in Ref. 3 obtained in the limit of short-correlated forcing. A different scaling is found for smaller values of $\xi<10^{-4}$ corresponding to the strong shear limit and a forcing with finite correlation time due to resonance, where the dotted fitted line exhibits logarithmic dependence on ξ as $\ln \xi$. The factor outside the integral (Ω_0^{-2}) then gives the inverse cascade $(\nu_T<0)$ in 2D HD turbulence with turbulent viscosity $\nu_T \propto \Omega_0^{-3}\ln\Omega_0$ in this limit.

As noted in Sec. I, a shear flow acts to elongate and disrupt turbulent eddies, quenching turbulent transport. This process is shown in Fig. 4 which shows the evolution in time of a 2D turbulent eddy in the presence of a fixed prescribed background shear flow. This distortion and ultimate breakup of turbulent eddies is responsible for the reduction in turbulent viscosity by flow shear seen here. Note that in our model there is no direct interaction between equilibrium shear flow and magnetic field such as phase-mixing discussed in Refs. 10–12. The stronger reduction with a forcing of finite correlation time is attributable to the more consistent movement of the turbulent flow which allows the shear flow more time to distort and disrupt turbulent eddies. That is, the fluid driven by random forcing with short correlation time moves

Downloaded 10 Aug 2011 to 194.81.223.66. Redistribution subject to AIP license or copyright; see http://pop.aip.org/about/rights_and_permissions

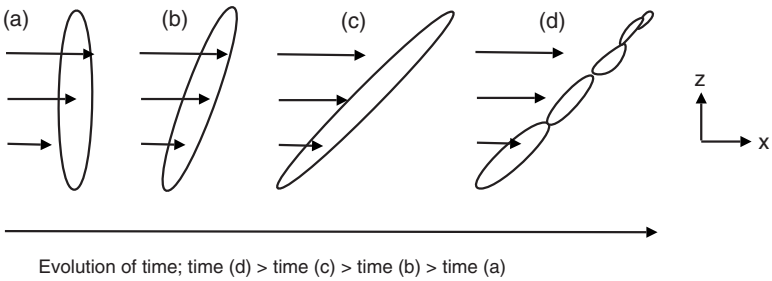

FIG. 4. Time evolution of a turbulent eddy subject to a shear flow $\mathbf{v}=V(z)\hat{x}$.

too rapidly to be affected by shear elongation and disruption, compared to the case with a forcing with longer correlation time.

IV. MAGNETOHYDRODYNAMICS

We now consider the effect of shear and magnetic field on turbulent transport in 2D MHD by including the Lorentz force in Eq. (1). For simplicity we assume $\nu=D$ and consider the limit of strong background magnetic field, where the parameter $B_\gamma=k_xB/\Omega_0=\xi M\gg 1$, i.e., the Alfvén frequency is large compared with the shearing rate. It can been seen that the parameter $M=Bk_x/k_x^2\nu$ is proportional to the Alfvén frequency Bk_x. Note that the case of nonunit magnetic Prandtl number has been investigated in previous work; see Ref. 13.

A. Turbulent diffusivity

By using solutions given in Eqs. (46) and (47) of Ref. 3, together with the correlation functions defined in Eqs. (16) and (17), we can obtain the equation for the magnetic flux as

$$\langle a'v_z'\rangle = \frac{\nu}{(2\pi)^2 B\Omega_0}\int d\mathbf{k}\frac{\hat{\phi}(\mathbf{k})}{k_x^2+k_z^2}e^{2\xi(k_z/k_x+1/3(k_z/k_x)^3)}I_{\mathrm{MF}},$$

$$I_{\mathrm{MF}} = \int_0^\infty\int_0^\infty d\tau_2 d\tau_1 \psi_0^2 \frac{\sin\varphi(\tau_1)}{\sqrt{(1+\tau_1^2)}}\frac{\sin\varphi(\tau_2)}{\sqrt{(1+\tau_2^2)}} \times \xi(2+\tau_1^2+\tau_2^2)e^{n(\tau_1,\tau_2)}. \tag{20}$$

Here we define

$$n(\tau_1,\tau_2) = \bar{\chi}(\tau_1)+\bar{\chi}(\tau_2)-\xi(Q(\tau_1)+Q(\tau_2)) - i(\bar{\omega}-k_x)(\tau_1-\tau_2)-\bar{\gamma}|\tau_1-\tau_2|,$$

$$\psi_0 = \left[1-\frac{1}{2B_\gamma^2}\right]^{-1},$$

$$\psi(\tau) = \left[1-\frac{1}{2B_\gamma^2(1+\tau^2)^2}\right]^{-1},$$

$$\bar{\chi}(\tau) = \frac{1}{4B_\gamma^2}\left[\frac{1}{(1+\tau^2)^2}-1\right], \tag{21}$$

$$\varphi(\tau) = B_\gamma\tau - \frac{1}{4B_\gamma}\left[\arctan\tau+\frac{\tau}{1+\tau^2}\right],$$

$$A(\tau) = \frac{-\tau\psi^2(\tau)\sin\varphi(\tau)}{B_\gamma(1+\tau^2)^{3/2}}+\frac{\cos\varphi(\tau)}{\sqrt{(1+\tau^2)}\psi(\tau)}.$$

The double integral over τ_i for $i=1,2$ for I_{MF} in Eq. (20) is carried out in exactly the same way as done in Sec. III, by using a fixed wavenumber $k_x=20.0$ and a decorrelation rate of $\hat{\gamma}=10^2$. Figure 5 shows I_{MF} as a function of $\bar{\omega}$ for fixed values of $M=10^{10}$ and $\xi=10^{-8}$. The peak in Fig. 5 is due to resonance where $\omega=k_x\Omega_0\pm k_xB$ (i.e., $\bar{\omega}=k_x\pm B_\gamma$). Thus, for the following numerical computation of I_{MF} the value of the turbulent frequency ω is chosen to be the value giving this maximum transport via resonance.

Figure 6 shows these results for different values of ξ and M. Panel (a) is obtained by varying shearing rates over $10^{-6}<\xi<10^{-1}$ for magnetic field strength $M=10^8$; panel (b) is by varying magnetic field strength over $10^6<M<10^{10}$ for shear strength $\xi=5\times10^{-5}$. In Fig. 6(a), the asymptotic fit to I_{MF} plotted by the dashed line in the regime $\xi>10^{-3}$ (weak shear strength and a short correlated forcing) shows a scaling of $\xi^{-1/3}$. The dotted line in Fig. 6(a) is a fit to the results in the region $\xi<10^{-4}$ (strong shear and a forcing of finite correlation time), which has a different scaling of $\xi^{1/4}$. In comparison, Fig. 6(b), I_{MF} in Eq. (20), shows no dependence on magnetic field across a wide range of B. With the incorporation of the factor outside I_{MF} in Eq. (20), namely, $B^{-1}\Omega_0^{-1}$, Eq. (15) then gives a quenching of turbulent diffusivity of $D_T\propto\Omega_0^{-2/3}B^{-2}$ in the delta correlated limit (in agreement with the analytical result found in Ref. 3) but a stronger reduction of $D_T\propto\Omega_0^{-5/4}B^{-2}$ in the case of the forcing with finite correlation time.

The reduction of turbulent magnetic diffusivity is basically due to the back-reaction of magnetic fields which are frozen into the fluid when $D=0$ in MHD (see, for example, Refs. 1–3). That is, as magnetic field is advected by a turbulent plasma the tension force of the magnetic field, which was initially negligible, increases, eventually reaching a point where it "snaps" the field line back towards its original position (Alfvénization), reducing turbulent transport. This

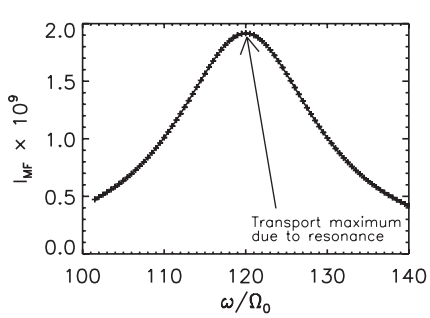

FIG. 5. I_{MF} in Eq. (20) plotted against turbulent frequency. The peak represents maximum transport due to resonance where $\bar{\omega}=k_x\pm B_\gamma$.

Downloaded 10 Aug 2011 to 194.81.223.66. Redistribution subject to AIP license or copyright; see http://pop.aip.org/about/rights_and_permissions

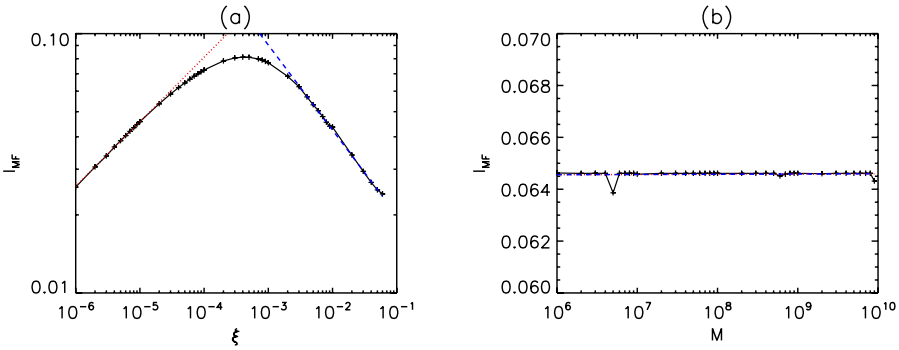

FIG. 6. (Color online) Dependence of I_{MF} in Eq. (20) on shearing rate ξ and magnetic field strength $M \propto B$.

reduction is more severe for a stronger magnetic field causing a greater suppression of turbulent transport.

The result of $D_T \propto B^{-2}$ holds for a broad range of ξ with or without resonance. This is an interesting result, illustrating that the resonance mainly affects shear flow suppression. The stronger suppression of D_T by shear flow in the case of a forcing with a finite correlation time is again attributed to the more consistent movement of the flow, which allows the shear flow more time in which to elongate and ultimately disrupt eddies.

B. Turbulent viscosity

Using the same method as for Eq. (20), the Reynolds and Maxwell stresses in the 2D MHD case are

$$\langle v_x' v_z' \rangle, \langle b_x' b_z' \rangle = \frac{-1}{(2\pi)^2 \Omega_0^2} \int d\mathbf{k} \frac{\hat{\phi}(\mathbf{k})}{k_x^2 (k_x^2 + k_z^2)} \times e^{2\xi[k_z/k_x + 1/3(k_z/k_x)^3]} \times I_{RS}, I_{MS}, \tag{22}$$

$$I_{RS} = \int_0^\infty \int_0^\infty d\tau_2 d\tau_1 \psi_0^2 \tau_1 A(\tau_1) A(\tau_2) e^{n(\tau_1,\tau_2)},$$

$$I_{MS} = \int_0^\infty \int_0^\infty d\tau_2 d\tau_1 \psi_0^2 \tau_1 \frac{\sin \varphi(\tau_1)}{\sqrt{(1+\tau_1^2)}} \frac{\sin \varphi(\tau_2)}{\sqrt{(1+\tau_2^2)}} e^{n(\tau_1,\tau_2)}. \tag{23}$$

Note that the total stress is given by the difference between these two as $\langle v_x' v_z' - b_x' b_z' \rangle$. In Eqs. (22) and (23) the same notations as in Eqs. (21) are used. Numerical integration is performed to obtain I_{RS} and I_{MS} by using a prescribed wavenumber $k_x = 20.0$ and a decorrelation rate of $\hat{\gamma} = 10^2$ and by choosing the turbulent frequency for maximum transport due to resonance $\bar{\omega} = k_x \pm B_\gamma$ (as per Secs. III and IV A).

Figures 7(a) and 7(b) show these results across the range of shear strengths $10^{-6} < \xi < 10^{-1}$ for a fixed value of magnetic field strength $M = 10^7$. The scaling found in the region of $\xi > 10^{-3}$, corresponding to weak shear strength and a short correlated forcing, is $\xi^{-1} \ln \xi$ (dashed line). The incorporation of the multiplicative factor of Ω_0^{-2} in the Reynolds stress and the Maxwell stress then gives us a logarithmic reduction as $\Omega_0^{-1} \ln \Omega_0$, in agreement with the analytic result of Ref. 3. In the region of $\xi < 10^{-4}$, with strong shear and a forcing of finite correlation time, a different scaling of approximately $\xi^{-1/3}$ is found (dotted line), leading to a quenching of both the Reynolds and Maxwell stresses as $\Omega_0^{-5/3}$ in this limit. The reduction in individual stress by shear flow is again a consequence of shear distortion and disruption of turbulent eddies, while a stronger reduction found in the case of a forcing with finite correlation time is due to the consistently similar movement of the flow giving the shear more time to affect eddies.

It is interesting to see that the two panels in Fig. 7 are both qualitatively and quantitatively similar, giving a small total stress $\langle u_x' u_z' - b_x' b_z' \rangle$. This is basically a consequence of Alfvénization of the flow, $\mathbf{u}' \sim \pm \mathbf{b}'$, in a strongly magnetized fluid (see, for example, Ref. 3). The small, residual total stress is due to imperfect Alfvénization resulting from effects such as dissipation, shear flow or resonance, as shown in Ref. 17. The scaling of the resulting turbulent viscosity for a short correlated forcing is numerically found to be B^{-2} in agreement with the analytic result of Ref. 3. Note that similar cancellation was also found in the case of nonunit magnetic Prandtl number, in Ref. 13. In the case of forcing with finite correlation time, $I_{RS} - I_{MS}$ is too small to permit the determination of the exact scaling of ν_T.

Figure 8 shows I_{RS} and I_{MS} in Eqs. (22) and (23) across

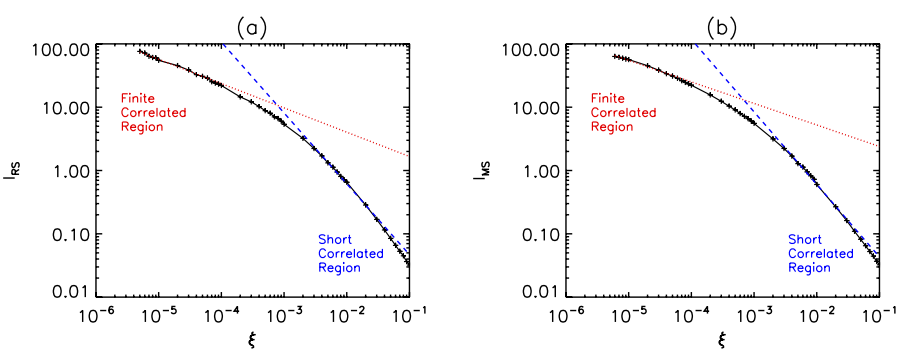

FIG. 7. (Color online) Dependence of I_{RS} and I_{MS} on shearing rate ξ. It can clearly be seen that they are both qualitatively and quantitatively the same.

Downloaded 10 Aug 2011 to 194.81.223.66. Redistribution subject to AIP license or copyright; see http://pop.aip.org/about/rights_and_permissions

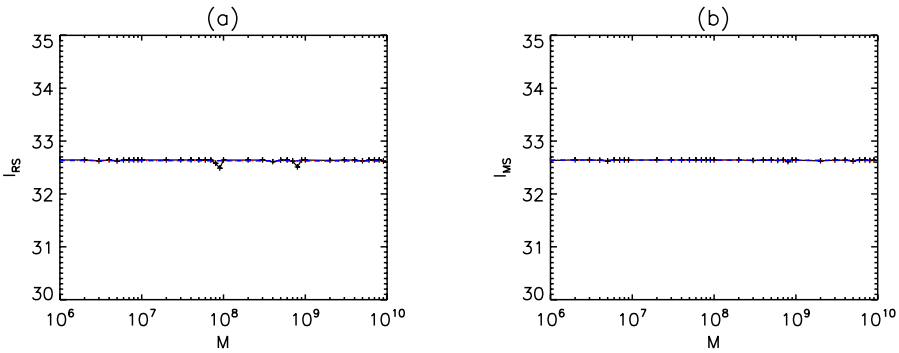

FIG. 8. (Color online) Dependence of I_{RS} and I_{MS} on magnetic field strength M, respectively. It is immediately clear they are both qualitatively and quantitatively the same.

a range of magnetic field strengths of $10^6 < M < 10^{10}$ for a fixed value of shear $\xi = 5 \times 10^{-5}$. It can clearly be seen that there is no dependence of the I_{RS} and I_{MS} over this wide range of magnetic field strengths. That is, magnetic field has no effect on the individual Reynolds and Maxwell stresses. Furthermore the values of I_{RS} and I_{MS} are almost indistinguishable, leading to small ν_T. This is true for all values of ξ and is again due to Alfvénization of the turbulence.

It should be noted that the results presented here allow the flow to be sheared but not the field. This may partially account for the fact that they have apparently different effects on the Reynolds and Maxwell stresses. In our model there are no natural instabilities of the relatively simple equilibrium fields considered. In more realistic situations, such effects could introduce new features outside the scope of the present investigation.

C. Amplitudes

We have found a significant reduction in transport (ν_T, D_T) due to B and Ω_0 in previous subsections. It is interesting to investigate where similar reduction appears in the amplitude (vigor) of the turbulence. By using the forcing Eqs. (16) and (17), the kinetic and magnetic energy can be obtained as

$$\langle v'^2 \rangle, \langle b'^2 \rangle = \frac{1}{(2\pi)^2 \Omega_0^2} \int d\mathbf{k} \frac{\hat{\phi}(\mathbf{k})}{k_x^2(k_x^2 + k_z^2)} e^{2\xi(k_z/k_x + 1/3(k_z/k_x)^3)} \times I_{KE}, I_{ME},$$

$$I_{KE} = \int_0^\infty \int_0^\infty d\tau_2 d\tau_1 \psi_0^2 \tau_1 \tau_2 A(\tau_1) A(\tau_2) e^{n(\tau_1,\tau_2)}, \tag{24}$$

$$I_{ME} = \int_0^\infty \int_0^\infty d\tau_2 d\tau_1 \psi_0^2 \tau_1 \tau_2 \frac{\sin \varphi(\tau_1)}{\sqrt{(1+\tau_1^2)}} \frac{\sin \varphi(\tau_2)}{\sqrt{(1+\tau_2^2)}} e^{n(\tau_1,\tau_2)}. \tag{25}$$

To find the dependence of kinetic and magnetic energy on large scale shear and magnetic field, I_{KE} and I_{ME} in Eqs. (24) and (25) are numerically computed in the same way as was done in Secs. III, IV A, and IV B, by using $k_x = 20.0$ and $\hat{\gamma} = 10^2$ and by selecting turbulent frequency for maximum amplitude due to resonance ($\bar{\omega} = k_x \pm B_\gamma$, as in Secs. III, IV A, and IV B).

Figure 9 shows the numerical results of I_{KE} and I_{ME} in Eqs. (24) and (25) across the range $10^{-6} < \xi < 10^{-1}$ for fixed magnetic field $M = 10^7$. The scaling of the dashed lines for larger values of $\xi > 10^{-3}$ (weak shear and a short correlated forcing) in both panels is $\xi^{-4/3}$, giving a reduction in magnetic and kinetic energies in Eqs. (24) and (25) as $\Omega_0^{-2/3}$ due to shear, in agreement with the short correlated forcing results of Ref. 3. This reduction is caused by enhanced dissipation of energy due to the formation of smaller scales by shearing. The dotted lines in Fig. 9 show a scaling of $\xi^{-2/3}$ for smaller values of $\xi < 10^{-4}$ (strong shear and a forcing of finite correlation time) giving a scaling of magnetic and kinetic energies in Eqs. (24) and (25) as $\Omega_0^{-4/3}$. We note that this reduction is stronger than that in the limit of weak shear and short correlated forcing, similar to the case of D_T and ν_T in Secs. III, IV A, and IV B.

To examine the effect of magnetic field on the kinetic and magnetic energies, I_{KE} and I_{ME} of Eqs. (24) and (25) were computed over the range $10^6 < M < 10^{10}$ for fixed shear $\xi = 5 \times 10^{-5}$. The results are shown in Fig. 10. No dependence of I_{KE} or I_{ME} on M in Fig. 10 clearly shows that kinetic and

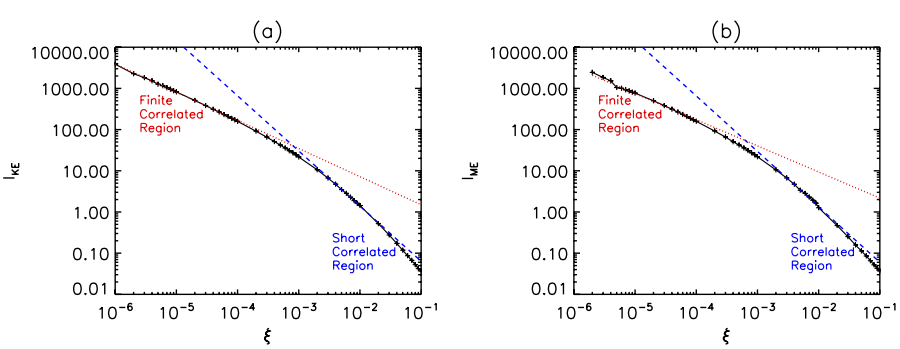

FIG. 9. (Color online) Dependence of I_{KE} and I_{ME} on shearing rate ξ.

Downloaded 10 Aug 2011 to 194.81.223.66. Redistribution subject to AIP license or copyright; see http://pop.aip.org/about/rights_and_permissions

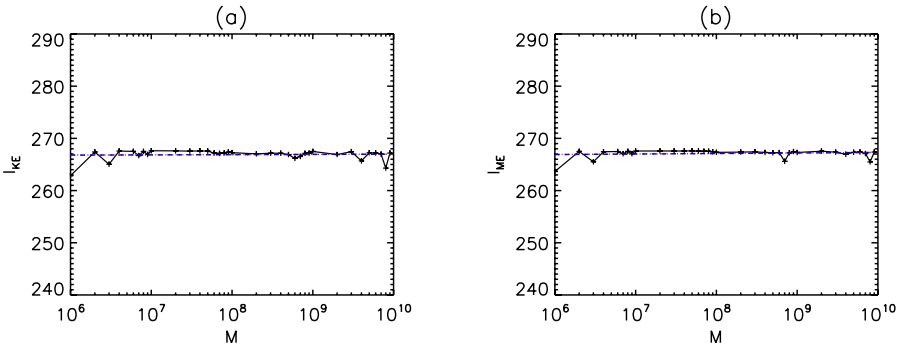

FIG. 10. (Color online) Dependence of I_{KE} and I_{ME} in Eqs. (24) and (25) on magnetic field strength M.

magnetic energy in Eqs. (24) and (25) are independent of B. It is simply because Alfvén waves due the magnetic field do not necessarily alter turbulence intensity. This result holds in both the cases with short and finite correlated forcing.

It is interesting to compare these results to D_T which is severely quenched not only by Ω_0 but also by B. This manifests a fundamental difference between the effects of shear and magnetic field on turbulence quenching. That is, while magnetic field quenches turbulent transport by Alfvénization without necessarily altering turbulence level, flow shear can reduce both transport and turbulence level by enhanced dissipation followed by eddy distortion and break up. It is also interesting to note that I_{KE} and I_{ME} are qualitatively and quantitatively similar, suggesting the almost equipartition between kinetic and magnetic energies due to Alfvénization. Note that similar results were found for the Reynolds and Maxwell stresses in Sec. IV B.

It is worth noting that in many applications kinetic energy $\langle u'^2\rangle$ and magnetic energy $\langle b'^2\rangle$ may be measured, our prediction can provide a route through which to determine the power spectrum of the forcing defined in Eq. (17). This can in turn be used to quantify the turbulent momentum transport ν_T and the turbulent magnetic diffusivity D_T.

V. CONCLUSION

We have investigated the effect of large scale magnetic field in parallel with large scale shear flow on the turbulent magnetic diffusivity and turbulent viscosity (momentum transport) in 2D HD and MHD turbulence, driven by a small-scale forcing with finite correlation time. In the MHD case we have considered the case of a unit Prandtl number ($\nu=D$).

In the case of HD turbulence, turbulent viscosity was found to be more strongly suppressed by a flow with a forcing of finite correlation time as $\nu_T \propto -\Omega_0^{-3}\ln\Omega_0$ compared to the case with a delta-correlated forcing where $\nu_T \propto -\Omega_0^{-2}$. In both cases, an inverse cascade persists.

In the case of MHD turbulence, magnetic diffusivity was found to be suppressed by magnetic field and shear as $D_T \propto B^{-2}\Omega_0^{-2/3}$ in the limit of a delta-correlated forcing (in agreement with Ref. 3), while in the limit of a forcing with finite correlation time it is more strongly quenched as $D_T \propto B^{-2}\Omega_0^{-5/4}$. In comparison, Reynolds and Maxwell stress, the difference between which is responsible for transport of momentum, are each found to be suppressed by shear flows only, being unaffected by the magnetic field. Specifically in the limit of a delta-correlated forcing, $\langle v_x' v_z'\rangle \propto \Omega_0^{-1}\ln\Omega_0$, while in the limit of a forcing of finite correlation time $\langle v_x' v_z'\rangle \propto \Omega_0^{-5/3}$. The same result holds for the Maxwell stress $\langle b_x' b_z'\rangle$. The Reynolds stress is cancelled by almost equal Maxwell stress with a small total stress $\langle v_x' v_z' - b_x' b_z'\rangle \approx 0$. Consequently the overall turbulent momentum transport is confirmed to be massively reduced. Similarly, kinetic and magnetic energy are found to be reduced by shear only, with the scaling $\langle v'^2\rangle$, $\langle b'^2\rangle \propto \Omega_0^{-2/3}$ in the limit of a short correlated forcing and $\langle v'^2\rangle$, $\langle b'^2\rangle \propto \Omega_0^{-4/3}$ in the limit of a forcing with finite correlation time. It is also noted that the values of magnetic and kinetic energies are found to be almost the same, providing additional evidence for the Alfvénization of turbulence.

All the scalings we have found for the transport coefficients due to magnetic field and shear are summarized in Table I. These results not only demonstrate the crucial effect of shear flow and magnetic field on turbulence regulation but also highlight the important difference in their effects. In all the cases a stronger reduction by flow shear was found for the case of the forcing with finite correlation time, despite the resonance. This suggests the importance of the property of the turbulent flow in flow shear suppression.

The strong reduction of ν_T and D_T could be problematic in understanding fast magnetic dissipation/reconnection and momentum transport observed in astrophysical and laboratory plasmas. Alternatively, it suggests that other physical mechanisms should be explored beyond the present work to explain the observations. For instance, the two-fluid effect

TABLE I. Summary of the scalings of transport coefficients and turbulence level due to large scale shear flows with shearing rate Ω_0 and uniform magnetic fields of strength B.

	Forcing with a short correlation time	Forcing with a finite correlation time
Magnetic diffusivity, D_T	$B^{-2}\Omega_0^{-2/3}$	$B^{-2}\Omega_0^{-5/4}$
Turbulent viscosity (HD), ν_T	Ω_0^{-2}	$\Omega_0^{-3}\ln\Omega_0$
Turbulent viscosity (MHD), ν_T	B^{-2}	$<B^{-2}$
Reynolds stress (MHD), $\langle v_x' v_z'\rangle$	$\Omega_0^{-1}\ln\Omega_0$	$\Omega_0^{-5/3}$
Maxwell stress (MHD), $\langle b_x' b_z'\rangle$	$\Omega_0^{-1}\ln\Omega_0$	$\Omega_0^{-5/3}$
Kinetic energy, $\langle v'^2\rangle$	$\Omega_0^{-2/3}$	$\Omega_0^{-4/3}$
Magnetic energy, $\langle b'^2\rangle$	$\Omega_0^{-2/3}$	$\Omega_0^{-4/3}$

Downloaded 10 Aug 2011 to 194.81.223.66. Redistribution subject to AIP license or copyright; see http://pop.aip.org/about/rights_and_permissions

can weaken turbulence quenching (see, for example, Ref. 18). In particular, in tokamaks other kinetic effects, toroidal geometry (e.g., geodesic acoustic modes), high energy particles, impurities, etc. can all contribute to the enhanced transport, as shown in Refs. 19 and 20, which were not incorporated in the simple model adopted in the present paper. Further, it would be interesting to extend the present study to include other physical effects such as inhomogeneous turbulence, nonuniform magnetic fields or time-dependent shear flows, which can be caused by the back reaction of turbulence onto shear flows (for more, see Ref. 11). These issues will be addressed in future publications.

ACKNOWLEDGMENTS

The authors thank J. Anderson and N. Leprovost for useful comments. We also thank A. Newton for numerous helpful discussions.

This work was supported in part by the United Kingdom Engineering and Physical Sciences Research Council and by the European Communities under the Contract of Association between EURATOM and UKAEA. The views and opinions expressed herein do not necessarily reflect those of the European Commission.

[1] F. Canttaneo and S. I. Vainshtein, Astrophys. J. Lett. **376**, L21 (1991).
[2] A. V. Gruziov and P. H. Diamond, Phys. Plasmas **3**, 1853 (1996).
[3] E. Kim and B. Dubrulle, Phys. Plasmas **8**, 813 (2001).
[4] K. H. Burrell, Phys. Plasmas **4**, 1499 (1997).
[5] E. Kim and P. H. Diamond, Phys. Rev. Lett. **90**, 185006 (2003).
[6] E. Kim, Mod. Phys. Lett. B **18**, 551 (2004).
[7] E. Kim, Astron. Astrophys. **441**, 763 (2005).
[8] E. Kim, Phys. Plasmas **13**, 022308 (2006).
[9] E. Kim and P. H. Diamond, Phys. Rev. Lett. **91**, 075001 (2003).
[10] A. Thyagaraja, N. Loureiro, and P. J. Knight, J. Plasma Phys. **68**, 363 (2002).
[11] A. Thyagaraja, P. J. Knight, and N. Loureiro, Eur. J. Mech. B/Fluids **23**, 475 (2004).
[12] E. Parker and A. Thyagaraja, Sol. Phys. **189**, 45 (1999).
[13] E. Kim, Phys. Rev. Lett. **96**, 084504 (2006).
[14] A. P. Newton and E. Kim, Phys. Plasmas **14**, 122306 (2007).
[15] M. Leconte, P. Beyer, S. Benkadda, and X. Garbet, Phys. Plasmas **13**, 112301 (2006).
[16] W. H. Press, B. P. Flannery, S. A. Teukolsky, and W. T. Vetterling, *Numerical Recipes (Fortran)* (Cambridge University Press, Cambridge, 1992).
[17] N. Miyato, Y. Kishimoto, and J. Li, Phys. Plasmas **11**, 5557 (2004).
[18] E. Kim, Phys. Rev. E **76**, 025401 (2007).
[19] B. Scott, New J. Phys. **7**, 92 (2005).
[20] V. Naulin, Phys. Plasmas **12**, 052515 (2005).

Downloaded 10 Aug 2011 to 194.81.223.66. Redistribution subject to AIP license or copyright; see http://pop.aip.org/about/rights_and_permissions